Ceramics International xxx (xxxx) xxx–xxx

Contents lists available at ScienceDirect

Ceramics International

journal homepage: www.elsevier.com/locate/ceramint

Facile synthesis of porous hollow Co_3O_4 microfibers derived-from metal-organic frameworks as an advanced anode for lithium ion batteries

Yingying Chen[a,b], Yue Wang[a], Hongxun Yang[a,b,*], Hui Gan[a], Xingwei Cai[a,b], Xingmei Guo[a], Bo Xu[c], Minfeng Lü[a,b], Aihuai Yuan[a,b]

[a] School of Environmental & Chemical Engineering, Jiangsu University of Science and Technology, Zhenjiang 212003, Jiangsu, China
[b] Marine Equipment and Technology Institute, Jiangsu University of Science and Technology, Zhenjiang 212003, Jiangsu, China
[c] School of Chemistry & Chemical Engineering, Jinan University, Jinan 250022, Shandong, China

A R T I C L E I N F O

Keywords:
Porous materials
Co_3O_4
Microfibers
Anode
Lithium ion batteries

A B S T R A C T

Co_3O_4, as a promising anode material for the next generation lithium ion batteries to replace graphite, displays high theoretical capacity (890 mAh g^{-1}) and excellent electrochemical properties. However, the drawbacks of its poor cycle performance caused by large volume changes during charge-discharge process and low initial coulombic efficiency due to large irreversible reaction impede its practical application. Herein, we have developed a porous hollow Co_3O_4 microfiber with 500 nm diameter and 60 nm wall thickness synthesized via a facile chemical precipitation method with subsequent thermal decomposition. As an advanced anode for lithium ion batteries, the porous hollow Co_3O_4 microfibers deliver an obviously enhanced electrochemical property in terms of lithium storage capacity (1177.4 mA h g^{-1} at 100 mA g^{-1}), initial coulombic efficiency (82.9%) and cycle performance (76.6% capacity retention at 200th cycle). This enhancement could be attributed to the well-designed microstructure of porous hollow Co_3O_4 microfibers, which could increase the contact surface area between electrolyte and active materials and accommodate the volume variations via additional void space during cycling.

1. Introduction

Lithium-ion batteries (LIBs) are the most popular power sources for electric vehicles, hybrid electric vehicles and portable electronic devices because of their high energy, high voltage, no memory effect, and long service life, etc. [1–9]. During the process of seeking LIBs with high performance, transitional metal oxides with superior theoretical capacities compared to commercial graphite, such as Co_3O_4 [10–30], Fe_2O_3 [31–34], SnO_2 [35,36], and etc., are considered to be promising anode materials because of their excellent physical and chemical properties. Especially for Co_3O_4, as one of the most promising anode material for the next generation LIBs to replace graphite, displays excellent electrochemical properties and high theoretical capacity (890 mA h g^{-1}) [10]. However, the drawback of its poor capacity retention caused by large volume changes during cycling frustrates its practical application [10–13]. To overcome the disadvantage of Co_3O_4 as anode, various nanostructures of Co_3O_4 have previously been fabricated, such as nanoparticles [16,17], nanofibers [18–23], nanoboxes [14], nanotubes [25], nanosheets [26–29], and nanocages [30]. Among these materials, one-dimensional (1D) cobalt oxides have received growing attentions. It is well known that 1D geometries with a highly accessible surface area allow efficient 1D electron transport along the longitudinal direction [19]. On the other hand, metal-organic frameworks (MOFs) are a class of organic-inorganic functional hybrid with large surface area and high porosity. The morphologies and pore sizes of MOFs can be tuned upon the selection of different organic bridging ligands and transition metal ions, and the porosity can offer a fast and convenient access to income and leave small molecules and ions in the transformation process [37–41]. Recently, MOFs as sacrificial templates have been designed to fabricate porous metal oxides or carbon nanostructures through thermal decomposition under controlled temperature and atmospheres [37–42]. Porous hollow structure could shorten Li^+ ion diffusion lengths, accommodate the volume variations, and improve the surface area between electrode and electrolyte during cycling [43,44]. However, some formed porous Co_3O_4 products failed to maintain original morphologies of the precursor, probably due to a lack of suitable templates or optimal synthetic conditions [5]. Therefore, it is still a great challenge to synthesize porous hollow Co_3O_4 with high surface area and specific morphology as anode materials for high

* Corresponding author.
E-mail address: yhongxun@126.com (H. Yang).

http://dx.doi.org/10.1016/j.ceramint.2017.05.004
Received 21 January 2017; Received in revised form 14 April 2017; Accepted 1 May 2017

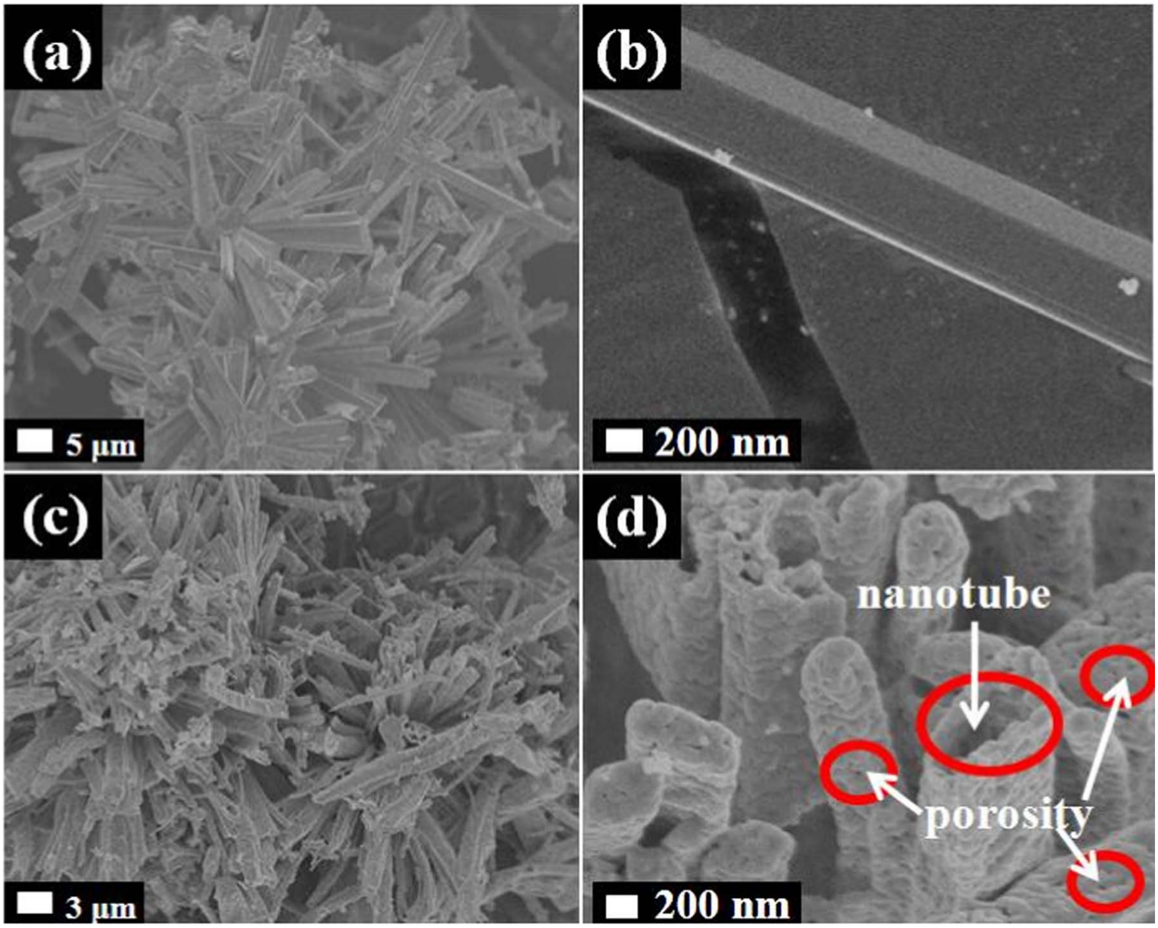

Fig. 1. SEM images of Co-MOF microfibers in low (a) and high (b) magnification. SEM images of porous Co_3O_4 microfibers in low (c) and high magnification (d).

performance lithium ion batteries.

Herein, we firstly report on the porous hollow Co_3O_4 microfibers synthesized via a facile chemical precipitation method followed by the thermal treatment. The chemical precipitation is a promising method to synthesize materials due to its advantages such as lower cost, less equipment requirements and easily controllable and scalable process [10,11]. The designed microstructure of porous hollow Co_3O_4 microfibers could increase the contact surface area between electrolyte and active materials, and accommodate the volume variations via additional void space during cycling, resulting in the obvious improvement in lithium storage capacity and cycle stability.

2. Experimental section

2.1. Preparation of porous Co_3O_4 microfibers

In a typical synthesis, 1 mmol cobalt (II) acetate monohydrate and 0.5 mmol L-glutamic acid were dissolved in 40 ml deionized water and stirred at ambient condition for 30 min. After that, 0.67 mmol 1, 3, 5-benzenetricarboxylic acid dissolved in 30 ml of ethanol was poured into the above solution under stirring. The solution turns turbid due to the formation of cobalt-based metal organic frameworks (Co-MOF) product. After stirring for 24 h at ambient condition, the pink precipitates were collected by centrifugation and washed three times with ethanol and distilled water. Then the Co-MOF product was dried and subsequently heated in a tube furnace under air flow with a ramp rate of 2 °C min^{-1}. It was maintained at 550 °C for 2 h and then naturally cooled down. The obtained sample was denoted as porous hollow Co_3O_4 microfibers.

2.2. Materials characterization

The morphologies and structures of the Co_3O_4 product were characterized with SEM (JEOL, JSM-6700F, 5 kV) and X-ray diffraction analyzer (Shimadzu XRD-6000 diffractometer using Cu-Kα radiation (0.15406 nm)). Energy-dispersive X-ray (EDX) analysis was performed on the Co_3O_4 product using the energy-dispersive X-ray spectroscopy attached to the JSM-6700F. The BET surface area was calculated from nitrogen adsorption data determined at 77 K using an ASAP 2020 surface analyzer. X-ray photoelectron spectroscopy (XPS) of the product was performed on a Perkin-Elmer model PHI 5600 system with a monochromatic Kα radiation (1486.6 eV) X-ray source.

2.3. Electrochemical measurements

For the preparation of the working electrodes, the porous hollow Co_3O_4 product (80 wt%), Super P (10 wt%), and polyvinylidene fluoride binder (10 wt%, Aldrich) were mixed and dissolved in N-methyl-2-pyrrolidinone to form a slurry. The slurry was coated on clear copper foil and dried at 80 °C in a vacuum oven for overnight. The active mass loading on the electrode is about 0.91 mg cm^{-2}. 2032 coin-type half-cells, the porous hollow Co_3O_4 product as working electrode, lithium foil as counter electrode, a Celgard 2250 film as separator and 1 M $LiPF_6$ in ethylene carbonate/diethyl carbonate (EC/DEC, 1:1 vol%) as electrolyte, were fabricated to evaluate the electrochemical properties using a battery cycle tester (LAND CT-2001A, Wuhan, China). Cyclic voltammetry (CV) measurements were performed on the Co_3O_4 product as working electrode using an electrochemical workstation (CHI 660E, Chenhua Ltd. Co., China) between 3.0 and 0.01 vs (Li/Li^+)/V at a sweep rate of 0.2 mV s^{-1}. Electrochemical impedance spectro-

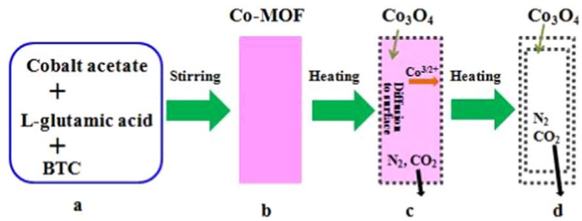

Fig. 2. Schematic of the fabrication procedure of porous Co_3O_4 microfibers. (a) Materials. (b) Co-MOF microfibers. (c) Formation of Co_3O_4 at the shell of Co-MOF in the thermal oxidation process. (d) Continual growth of Co_3O_4 microfibers from Co-MOF, which involves the nonequilibrium inter-diffusion, volume loss, and release of N_2 and CO_2, and eventual formation of the porous Co_3O_4 architectures.

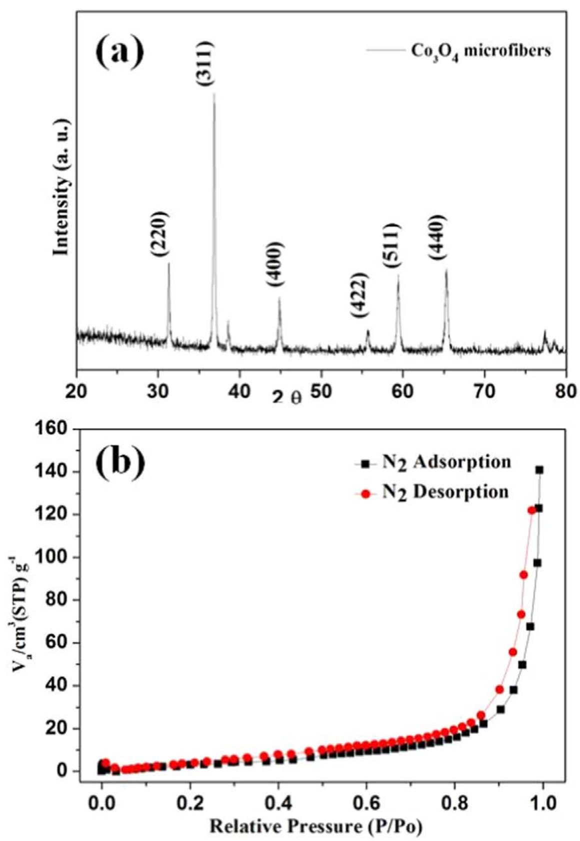

Fig. 3. (a) XRD patterns of the porous Co_3O_4 microfibers. (b) N_2 adsorption-desorption analysis of porous Co_3O_4 microfibers.

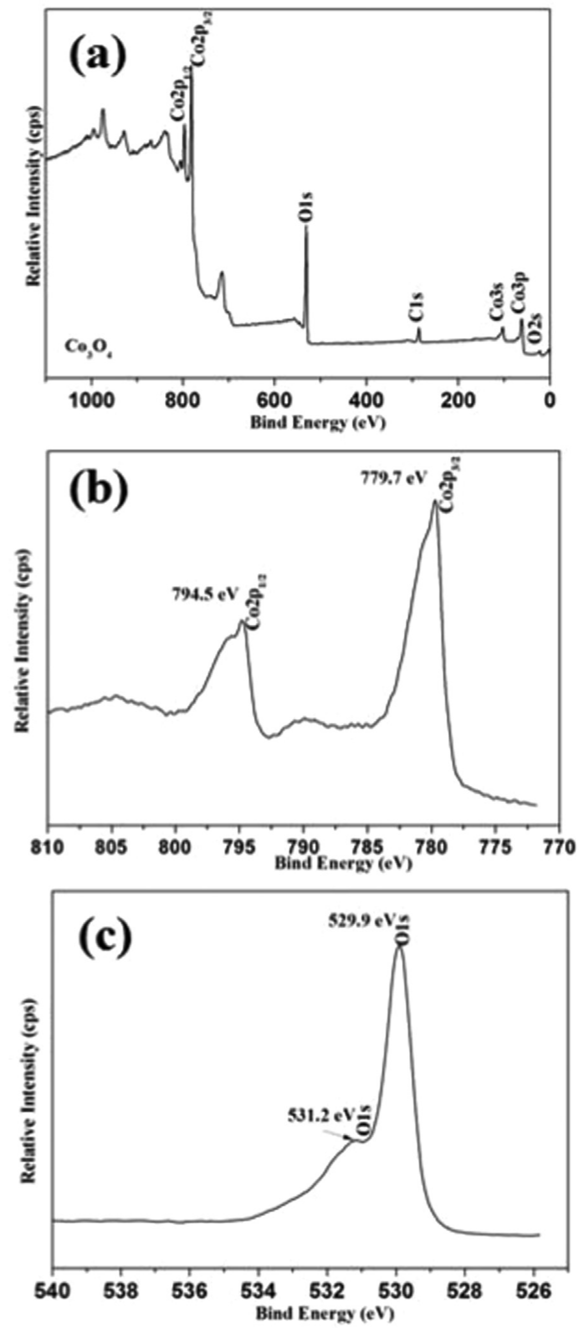

Fig. 4. XPS spectra of Co_3O_4: (a) full survey scans spectrum. (b) Co2p peaks. (c) O1s peaks.

scopy (EIS) tests were measured on an electrochemical workstation (Autolab PGSTAT 302N) operating in the frequency range of 0.01–10^5 Hz with ac amplitude of 10 mV.

3. Results and discussion

3.1. Characterizations of porous hollow Co_3O_4 microfibers

Fig. 1 exhibits the SEM images of Co-MOF and Co_3O_4 product. As seen in Fig. 1a and b, the Co-MOF fibers exhibit a long and straight morphology with about 600 nm diameter. After thermal treatment, the average diameter of porous hollow Co_3O_4 microfibers is about 500 nm (Fig. 1c), and the diameter distribution is narrow (Fig. S1). It is very interesting that the diameter of the porous hollow Co_3O_4 microfibers is smaller than that of its precursor Co-MOF. The particle size reduction was mainly caused by removing the organic parts during calcination. Owing to the volume loss and release of internally generated CO_2 and N_2 in the process of inter-diffusion, Co_3O_4 microfibers with 60 nm wall thickness form porosity and hollow morphology (Fig. 1d) [45,46]. In order to further check whether Co and O are in the as-prepared product, EDX analysis attached to SEM was also carried out (Fig. S2). The EDX spectrum in Fig. S2 confirms that the product contains Co and O elements, and no other elements are detected. The fabrication procedure of the porous hollow Co_3O_4 microfibers is exhibited in Fig. 2.

Fig. 3a shows the XRD patterns of the porous hollow Co_3O_4 microfibers. The dominant diffraction peaks can be indexed to the cubic phase of Co_3O_4 (JCPDS No. 03-065-3103). Characteristic peaks at 31.30°, 36.86°, 44.82°, 55.84°, 59.37°, and 65.35° correspond to the (220), (311), (400), (422), (511), and (440) diffraction planes, respectively [10]. No significant impurities or other phases were observed, which are consistent with the results of EDX. The surface areas and pore structures of the porous hollow Co_3O_4 product were further investigated using N_2 adsorption-desorption measurement. As seen in Fig. 3b, the adsorption isotherm forms a distinct hysteresis loop over

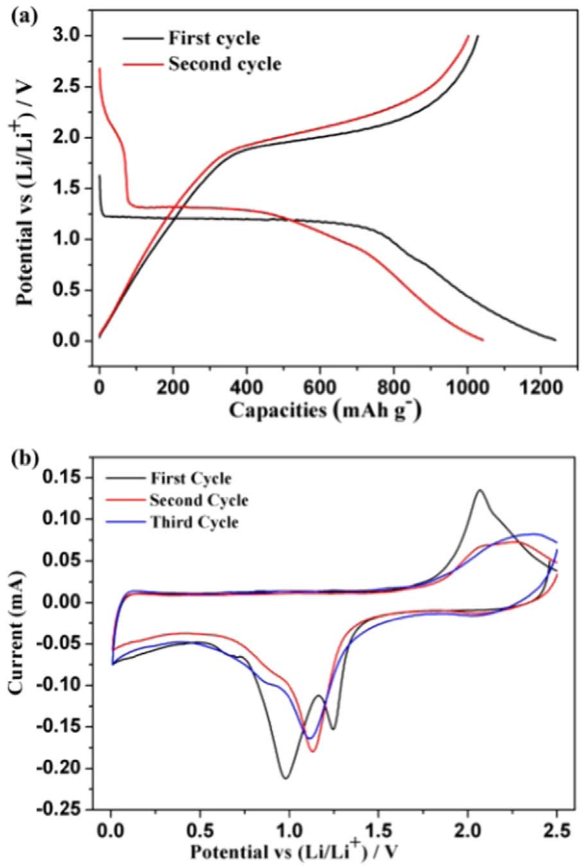

Fig. 5. (a) The discharge/charge voltage profiles of porous Co_3O_4 microfibers as anode in the range of 0.01–3.0 vs (Li/Li^+) V at 100 mA g^{-1} rate. (b) CV profiles for porous Co_3O_4 microfibers at a sweep rate of 0.2 mV s^{-1}.

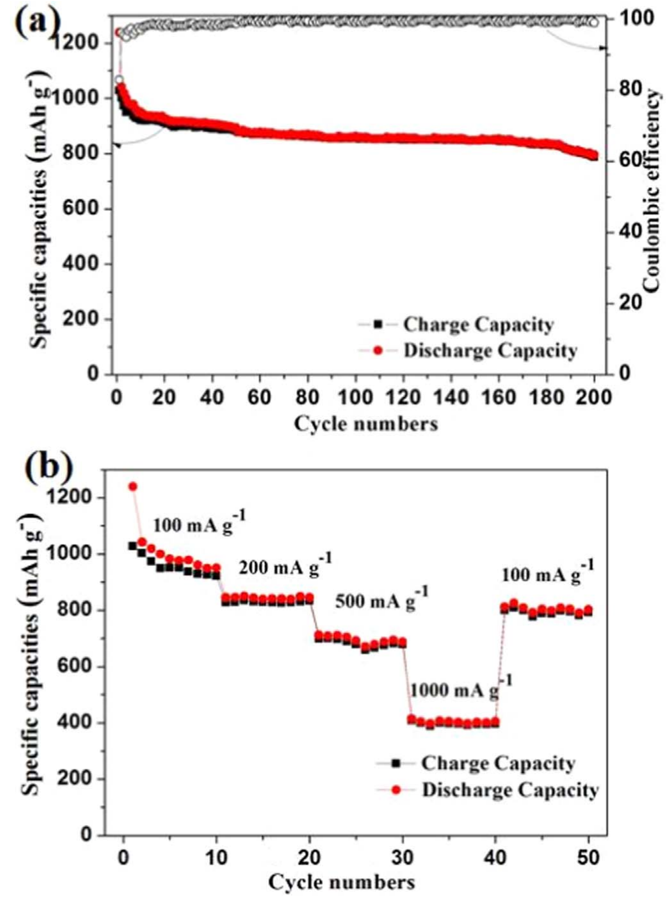

Fig. 6. (a) Cycle performances for porous Co_3O_4 microfibers as anode at a rate of 100 mA g^{-1}. (b) Rate capabilities of porous Co_3O_4 microfibers as anodes for LIBs at different rates.

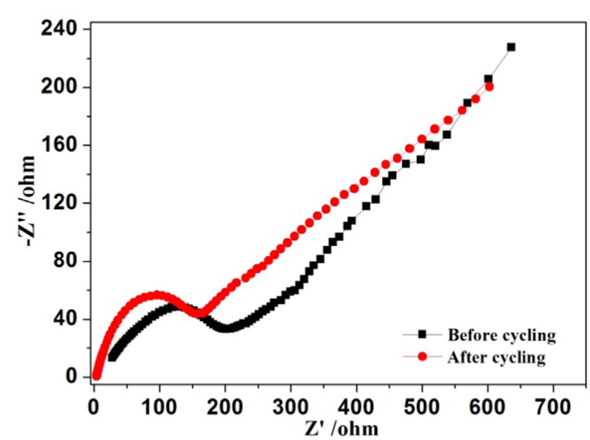

Fig. 7. EIS spectra of porous Co_3O_4 microfibers as anode for LIBs before cycling and after 100 cycles.

the range of $0.45 < P/P_0 < 0.95$, showing the typical mesoporous characteristics of Co_3O_4 microfibers [29]. The BET surface area and total pore volume of the porous Co_3O_4 microfibers were calculated to be 38.5 m^2 g^{-1} and 0.27 cm^3 g^{-1}, respectively. The larger surface area endows porous hollow Co_3O_4 microfibers with more lithium storage sites, while the mesoporous microstructure can facilitate the transportation of electrolyte molecules and Li^+ ions and relieve the volume change of the electrode materials during cycling. It can be expected that the porous hollow Co_3O_4 microfibers could deliver higher specific capacity and excellent capacity retentions.

In order to explore the surface component of the products, XPS of Co_3O_4 were measured. As exhibited in Fig. 4a, the peaks on the full patterns are mainly attributed to C1s (285.5 eV), O1s (529.9 eV) and Co2p (794.5 and 779.7 eV), showing the existence of carbon, oxygen, and cobalt element. It should be noted that the lower peak for C1s binding energy suggests that the products consist of C elements, which is from a small amount of residue of the decomposition of organic ligands. This phenomenon is very similar to previous report [11]. Fig. 4b shows that the Co2p XPS spectra present two major peaks centered at 794.5 and 779.7 eV, which can be attributed to Co2p1/2 and Co2p3/2 of the Co_3O_4. The O1s spectrum in the Fig. 4c also exhibit two peaks at 529.9 and 531.2 eV, indicating the lattice oxygen of spinel Co_3O_4 [11]. The XPS results are consistent with those of EDX and further prove that the as-synthesized product is Co_3O_4.

3.2. Electrochemical performances of porous Co_3O_4 microfibers

The electrochemical performance of porous hollow Co_3O_4 microfibers as anode for LIBs was evaluated by a standard half-cell testing system. Fig. 5a displays the discharge/charge curves of porous hollow Co_3O_4 microfibers for the first two cycles in the range of 0.01–3.0 vs (Li/Li^+) V. In the first discharge step, the porous Co_3O_4 microfibers exhibit a long voltage plateaus at 1.25 V and short one at 0.8 V, followed by a sloping curve down to 0.01 V. And in the first charge step, the Co_3O_4 exhibited a voltage plateaus at 2.25 V. The first discharge capacity for Co_3O_4 is about 1177.4 mAh g^{-1}, which is much higher than its theoretical capacity. This phenomenon is ascribed to the irreversible reaction of Co_3O_4 with Li^+ to form amorphous lithium oxide and a solid-electrolyte-interface (SEI) layer during the first cycle, which is very similar to those of transition metal oxides-based anodes [2,5–8]. The high surface area of the porous hollow Co_3O_4 microfibers might also contribute to the high irreversible capacity. It should be noted that the porous hollow Co_3O_4 microfibers delivered a higher initial coulombic efficiency (82.9%) than previous reports (73.8%) [19]. Fig. 5b exhibits the CV curves of porous hollow Co_3O_4 microfibers in the first three cycles scanned at 0.2 mV s^{-1} within the voltage window of 0.01–2.5 V vs. Li/Li^+. In the first cathodic scan, the peak at 1.26 V is ascribed to the formation of a SEI film, which is accordance with the first discharge curve. The 0.98 V peak is ascribed to the reduction reaction of Co_3O_4 with Li^+ and the formation of Li_2O. While in the charge process, the anodic peak around 2.05 V could be attributed to the oxidation reaction of Co to Co_3O_4. During the second cycle, a cathodic peak at 1.13 V and the corresponding anodic peak around 2.10 V are observed, resulting from the decomposition and formation of Co_3O_4. The electrochemical reactions for porous Co_3O_4 microfibers as anode are as follows:

$$Co_3O_4+8Li^++8e^-\leftrightarrow 4Li_2O+3Co^0 \quad (1)$$

$$8Li\leftrightarrow 8Li^++8e^- \quad (2)$$

The capacity retentions and the coulombic efficiency of the porous hollow Co_3O_4 microfibers are also evaluated by prolonging cycling over 200 cycles at a current density of 100 mA g^{-1} between 0.01 V and 3.0 V (Fig. 6a). As seen in Fig. 6a, the porous hollow Co_3O_4 microfibers still delivered a charge capacity of 787.6 mA h g^{-1} with capacity retention of 76.6% at 200th cycle, which is still much higher than the theoretical capacity of commercial graphite and previous reported [19–21]. This improvement may be attributed to the porous hollow microstructure of Co_3O_4 microfibers with additional void space which could accommodate the volume variations during cycling. Rate capabilities are also an important parameter for LIBs. Fig. 6b exhibits the rate capabilities of porous hollow Co_3O_4 microfibers at different current densities ranging from 100 to 1000 mA g^{-1} with each stage comprising 10 discharge/charge cycles. As shown in Fig. 6b, porous hollow Co_3O_4 microfibers exhibited decent capacity retention with an average charge capacity of 957.1, 829.7 , 683, and 397.6 mA h g^{-1} under the rate of 100, 200, 500 and 1000 mA g^{-1}, respectively. It should be noted that the porous Co_3O_4 microfibers delivered a 793.3 mA h g^{-1} charge capacity when the charge rate was returned to 100 mA g^{-1}, demonstrating the potential of porous hollow Co_3O_4 microfibers as a high rate anode for LIBs. The reason for this advanced performance may be that the 1D porous nanostructures could shorten the transport pathways of lithium ions and electrons, and reduce the diffusion length and resistance of the electrolyte molecules, resulting in the enhancement of rate capability.

To further understand lithium-storage properties, EIS of porous hollow Co_3O_4 microfibers were investigated on a fresh cell and after 100 cycles at 100 mA g^{-1}, as displayed in Fig. 7. The two Nyquist plots consist of one semicircle in the high-frequency region and a straight line in the low-frequency region. The semicircle portion is related to the reactions occurring on the electrode-electrolyte interface, which reflects the charge transfer impedance and SEI impedance. The larger the diameter of the semicircle, the larger the charge transfer resistance. It can be seen that the cell after cycling exhibit a smaller diameter of semicircle than the fresh cell, showing that the fresh cell has the higher charge transfer resistance. This result suggests that the higher diffusivity of lithium ions with increasing charge-discharge cycles can reduce the charge transfer resistance. In a word, the porous hollow Co_3O_4 microfibers show excellent electrochemical property, which could be explained as follows: firstly, the porous hollow microstructure of Co_3O_4 product could shorten the diffusion length of Li^+ ions and electrons resistance of the electrolyte molecules, resulting in improving the electrochemical kinetics. Secondly, the porous hollow microstructure of Co_3O_4 product could increase the contact surface between electrolyte and Co_3O_4 microfibers, thus improving the effective utilization of electrode materials. Thirdly, the porous hollow microstructure of Co_3O_4 product could accommodate the volume variation via additional void space during charge-discharging cycle.

4. Conclusions

In summary, porous hollow Co_3O_4 microfibers were firstly designed and synthesized via chemical precipitation with subsequent thermal treatment, a facile and scalable method. As an advanced anode for LIBs, the porous hollow Co_3O_4 microfibers exhibit an obviously enhanced electrochemical properties in terms of reversible capacity and cycle performance. This improvement is mainly attributed to the porous hollow microstructures of Co_3O_4 microfibers, which could increase the contact surface area between electrolyte and active materials and accommodate the volume variations of Co_3O_4 active material via additional void space during cycling.

Acknowledgments

This work was financially supported by the National Natural Science Foundation of China (21671185, 51672114), the Natural Science Foundation of the Jiangsu Higher Education Institution of China (14KJB150007), and the State Key Laboratory of Structural Chemistry of Fujian Institute of Research on the Structure of Matter (20150020).

Appendix A. Supporting information

Supplementary data associated with this article can be found in the online version at doi:10.1016/j.ceramint.2017.05.004.

References

[1] W.Y. Li, L.N. Xu, J. Chen, Co_3O_4 nanomaterials in lithium-ion batteries and gas sensors, Adv. Funct. Mater. 15 (2005) 851–857.
[2] L.W. Ji, Z. Lin, M. Alcoutlabi, X.W. Zhang, Recent developments in nanostructured anode materials for rechargeable lithium-ion batteries, Energy Environ. Sci. 4 (2011) 2682–2699.
[3] S.N. Sun, Y. Nie, M.C. Sun, T. Liang, M.F. Sun, H.X. Yang, Facile synthesis of $CoNi_2S_4$ one-dimensional nanorods as anode for high performance lithium ion batteries, Mater. Lett. 176 (2016) 87–90.
[4] H.X. Yang, L. Li, Tin-indium/graphene with enhanced initial coulombic efficiency and rate performance for lithium ion batteries, J. Alloy. Compd. 584 (2014) 76–80.
[5] V.A. Agubra, L. Zuniga, D. Flores, J. Villareal, M. Alcoutlabi, Composite nanofibers as advanced materials for Li-ion, Li-O_2 and Li-S Batteries, Electrochim. Acta 192 (2016) 529–550.
[6] V.A. Agubra, L. Zuniga, D.D. Garza, L. Gallegos, M. Pokhrel, M. Alcoutlabi, Forcespinning: a new method for the mass production of Sn/C composite nanofiber anodes for lithium ion batteries, Solid State Ion. 286 (2016) 72–82.
[7] V.A. Agubra, D.D. Garza, L. Gallegos, M. Alcoutlabi, Force spinning of polyacrylonitrile for mass production of lithium-ion battery separators, J. Appl. Polym. Sci. (2016). http://dx.doi.org/10.1002/APP.42847.
[8] L. Zuniga, V. Agubra, D. Flores, H. Campos, J. Villareal, M. Alcoutlabi, Multichannel hollow structure for improved electrochemical performance of TiO_2/carbon composite nanofibers as anodes for lithium ion batteries, J. Alloy. Compd. 686 (2016) 733–743.
[9] H.X. Yang, T.S. Song, L. Liu, A. Devadoss, F. Xia, H. Han, H. Park, W. Sigmund, K. Kwon, U. Paik, Polyaniline/polyoxometalate hybrid nanofibers as cathode for lithium ion batteries with improved lithium storage capacity, J. Phys. Chem. C 117 (2013) 17376–17381.
[10] J. Shao, Z.M. Wan, H.M. Liu, H.Y. Zheng, T. Gao, M. Shen, Q.T. Qu, H.H. Zheng, Metal organic frameworks-derived Co_3O_4 hollow dodecahedrons with controllable interiors as outstanding anodes for Li storage, J. Mater. Chem. A 2 (2014) 12194–12200.
[11] L.M. Zhang, B. Yan, J.H. Zhang, Y.J. Liu, A.H. Yuan, G. Yang, Design and self-assembly of metal-organic framework-derived porous Co_3O_4 hierarchical structures for lithium-ion batteries, Ceram. Int. 42 (2016) 5160–5170.
[12] B. Yan, L. Chen, Y.J. Liu, G.X. Zhu, C.G. Wang, J.H. Zhang, G. Yang, H.T. Ye, A.H. Yuan, Co_3O_4 nanostructures with a high rate performance as anode materials for lithium-ion batteries, prepared via book-like cobalt-organic frameworks, Crystengcom 16 (2014) 10227–10234.
[13] G. Huang, F.F. Zhang, X.C. Du, Y.L. Qin, D.M. Yin, L.M. Wang, Metal organic frameworks route to in situ insertion of multiwalled carbon nanotubes in co_3O_4 polyhedra as anode materials for lithium-ion batteries, ACS Nano 9 (2015) 1592–1599.
[14] J. Zhang, Z.Y. Lu, F. Zhang, L.J. Wang, P. Xiao, K.D. Yuan, M. Lai, W. Chen, Facile synthesis of hierarchical porous Co_3O_4 nanoboxes as efficient cathode catalysts for Li-O_2 batteries, J. Mater. Chem. A 4 (2016) 6350–6356.
[15] D.H. Ge, H.B. Geng, J.Q. Wang, J.W. Zheng, Y. Pan, X.Q. Cao, H.W. Gu, Porous nano-structured Co_3O_4 anode materials generated from coordination-driven self-assembled aggregates for advanced lithium ion batteries, Nanoscale 6 (2014)

9689–9694.
[16] J.J. Zhang, T. Huang, A.S. Yu, Synthesis and effect of electrode heat-treatment on the superior lithium storage performance of Co_3O_4 nanoparticles, J. Power Sources 273 (2015) 894–903.
[17] D.L. Wang, Y.C. Yu, H. He, J. Wang, W.D. Zhou, H.D. Abrun, Template-free synthesis of hollow-structured Co_3O_4 nanoparticles as high-performance anodes for lithium-ion batteries, ACS Nano 9 (2015) 1775–1781.
[18] X.Y. Yao, X. Xin, Y.M. Zhang, J. Wang, Z.P. Liu, X.X. Xu, Co_3O_4 nanowires as high capacity anode materials for lithium ion batteries, J. Alloy. Compd. 521 (2012) 95–100.
[19] H.X. Yang, Y. Wang, Y. Nie, S.N. Sun, T.Y. Yang, Co_3O_4/porous carbon nanofibers composite as anode for high-performance lithium ion batteries with improved cycle performance and lithium storage capacity, J. Compos. Mater. 51 (2017) 215–222.
[20] M.S. Uthanapillil, J. Feng, D. Aurélie, P.G. Bruce, Mesoporous and nanowire Co_3O_4 as negative electrodes for rechargeable lithium batteries, Phys. Chem. Chem. Phys. 9 (2007) 1837–1842.
[21] Y.G. Li, B. Tan, Y.Y. Wu, Mesoporous Co_3O_4 nanowire arrays for lithium ion batteries with high capacity and rate capability, Nano Lett. 8 (2008) 265–270.
[22] P. Zhang, Z.P. Guo, Y.D. Huang, D.Z. Jia, H.K. Liu, Synthesis of Co_3O_4/carbon composite nanowires and their electrochemical properties, J. Power Sources 196 (2011) 6987–6991.
[23] J. Chen, X.H. Xia, J.P. Tu, Q.Q. Xiong, Y.X. Yu, X.L. Wang, C.D. Gu, Co_3O_4-C core-shell nanowire array as an advanced anode material for lithium ion batteries, J. Mater. Chem. 22 (2012) 15056–15061.
[24] H.W. Song, L.S. Shen, C.X. Wang, Template-free method towards quadrate Co_3O_4 nanoboxes from cobalt coordination polymer nano-solids for high performance lithium ion battery anodes, J. Mater. Chem. A 2 (2014) 20597–20604.
[25] N. Du, H. Zhang, B.D. Chen, J.B. Wu, X.Y. Ma, Z.H. Liu, Y.Q. Zhang, D.R. Yang, X.H. Huang, J.P. Tu, Porous Co_3O_4 nanotubes derived from $Co_4(CO)_{12}$ clusters on carbon nanotube templates: a highly efficient material for Li-battery applications, Adv. Mater. 19 (2007) 4505–4509.
[26] W.L. Yao, J. Yang, J.L. Wang, Y. Nu, Multilayered cobalt oxide platelets for negative electrode material of a lithium-ion battery, J. Electrochem. Soc. 155 (2008) A903–A908.
[27] S.Q. Chen, Y.F. Zhao, B. Sun, Z.M. Ao, X.Q. Xie, Y.Y. Wei, G.X. Wang, Microwave-assisted synthesis of mesoporous Co_3O_4 nanoflakes for applications in lithium ion batteries and oxygen evolution reactions, ACS Appl. Mater. Interfaces 7 (2015) 3306–3313.
[28] H.X. Chen, Q.B. Zhang, J.X. Wang, D.G. Xu, X.H. Li, Y. Yang, K.L. Zhang, Improved lithium ion battery performance by mesoporous Co_3O_4 nanosheets grown on self-standing NiSix nanowires on nickel foam, J. Mater. Chem. A 2 (2014) 8483–8490.
[29] Y.H. Jin, L. Wang, Y.M. Shang, J. Gao, J.J. Lia, X.M. He, Facile synthesis of monodisperse Co_3O_4 mesoporous microdisks as an anode material for lithium ion batteries, Electrochim. Acta 151 (2015) 109–117.
[30] N. Yan, F. Wang, L. Hu, Y. Li, Y. Wang, L. Hu, Q.W. Che, Hollow porous SiO_2 nanocubes towards high-performance anodes for lithium-ion batteries, J. Phys. Chem. C 115 (2012) 7227–7235.
[31] Y.Y. Chen, R. Cai, Y. Yang, C. Liu, A.H. Yuan, H.X. Yang, X.P. Shen, Cyanometallic frameworks derived hierarchical porous Fe_2O_3/NiO microflowers with excellent lithium-storage property, J. Alloy. Compd. 698 (2017) 469–475.
[32] M.C. Sun, M.F. Sun, H.X. Yang, W.H. Song, Y. Nie, S.N. Sun, Porous Fe_2O_3 nanotubes as advanced anode for high performance lithium ion batteries, Ceram. Int. 43 (2017) 363–367.
[33] M.H. Chen, J.L. Liu, D.L. Chao, J. Wang, J.H. Yin, J.Y. Lin, H.J. Fan, Z.X. Shen, Porous α-Fe_2O_3 nanorods supported on carbon nanotubes-graphene foam as superior anode for lithium ion batteries, Nano Energy 9 (2014) 364–372.
[34] H.G. Wang, Y.Q. Zhou, Y. Shen, Y.H. Li, Q.H. Zuo, Q. Duan, Fabrication, formation mechanism and the application in lithium-ion battery of porous Fe_2O_3 nanotubes via single-spinneret electrospinning, Electrochim. Acta 158 (2015) 105–112.
[35] H.B. Wu, J.S. Chen, X.W. Lou, H.H. Hong, Synthesis of SnO_2 hierarchical structures assembled from nanosheets and their lithium storage properties, J. Phys. Chem. C 115 (2011) 24605–24610.
[36] H.X. Yang, T.S. Song, S.K. Lee, H.K. Han, F. Xia, A. Devadoss, W. Sigmund, U.Y. Paik, Tin indium oxide/graphene nanosheet nanocomposite as an anode material for lithium ion batteries with enhanced lithium storage capacity and rate capability, Electrochim. Acta 91 (2014) 275–281.
[37] H.L. Jiang, Q. Xu, Porous metal-organic frameworks as platforms for functional applications, Chem. Commun. 47 (2011) 3351–3370.
[38] L. Zhang, H.B. Wu, S. Madhavi, H.H. Hng, X.W. (David) Lou, Formation of Fe_2O_3 microboxes with hierarchical shell structures from metal-organic frameworks and their lithium storage properties, J. Am. Chem. Soc. 134 (2012) 17388–17391.
[39] M. Hu, A.A. Belik, M. Imura, K. Mibu, Y. Tsujimoto, Y. Yamauchi, Synthesis of superparamagnetic nanoporous iron oxide particles with hollow interiors by using prussian blue coordination polymers, Chem. Mater. 24 (2012) 2698–2707.
[40] R.B. Wu, X.K. Qian, F. Yu, H. Liu, K. Zhou, J. Wei, Y.Z. Huang, MOF-templated formation of porous CuO hollow octahedra for lithium-ion battery anode materials, J. Mater. Chem. A 1 (2013) 11126–11129.
[41] M. Huang, K. Mi, J.H. Zhang, H.L. Liu, T.T. Yu, A.H. Yuan, Q.H. Kong, S.L. Xiong, MOF-derived bi-metal embedded N-doped carbon polyhedral nanocages with enhanced lithium storage, J. Mater. Chem. A 5 (2017) 266–274.
[42] R.B. Wu, X.K. Qian, X.H. Rui, H. Liu, B. Ya, K. Zhou, J. Wei, Q.Y. Yan, X.Q. Feng, Y. Long, L.Y. Wang, Y.Z. Huang, Zeolitic imidazolate framework 67-Derived high symmetric porous Co_3O_4 hollow dodecahedra with highly enhanced lithium storage capability, Small 10 (2014) 1932–1938.
[43] S.X. Wang, S.L. Chen, Q.L. Wei, X.K. Zhang, S.Y. Wong, S.H. Sun, X. Li, Bioinspired synthesis of hierarchical porous graphitic carbon spheres with out-standing high-rate performance in lithium-ion batteries, Chem. Mater. 27 (2015) 336–342.
[44] R.B. Wu, X.K. Qian, K. Zhou, J. Wei, J. Lou, P.M. Ajayan, Porous spinel $Zn_xCo_{3-x}O_4$ hollow polyhedra templated for high-rate lithium-ion batteries, ACS Nano 8 (2014) 6297–6303.
[45] L. Hu, N. Yan, Q.W. Chen, P. Zhang, H. Zhong, X.R. Zheng, Y. Li, X.Y. Hu, Fabrication based on the Kirkendall effect of Co_3O_4 porous nanocages with extraordinarily high capacity for lithium storage, Chem. Eur. J. 18 (2012) 8971–8977.
[46] L. Hu, Q.W. Chen, Hollow/porous nanostructures derived from nanoscale metal-organic frameworks towards high performance anodes for lithium-ion batteries, Nanoscale 6 (2014) 1236–1257.